

An emerging many-body ergodic state between two classes of many-body localized states

Wai Pang Sze and Tai Kai Ng

Department of Physics, Hong Kong University of Science and Technology, Clear Water Bay, Hong Kong, China

In this paper, we report our numerical analysis of energy level spacing statistics for one-dimensional spin-1/2 XXZ model with random on-site longitudinal magnetic fields B_i . We concentrate on the strong disorder limit where the system is expected to be in either a *paramagnetic* many-body localized (MBL) state or a *spin-glass* MBL state. By analyzing the energy-level spacing statistics as a function of strength of random magnetic field h/J_\perp ($-h \leq B_i \leq h$), interaction strength J_z/J_\perp , energy of the many-body state E and the number of spin- \uparrow particles in the system $M = \sum_i (s_i^z + \frac{1}{2})$, we show that there exists a small region between the paramagnetic and spin-glass MBL phases where an ergodic phase emerges. The ergodic phase emerges at the middle of the many-body energy spectrum when $M \sim \frac{N}{2}$ and is *not* adiabatically connected to the ergodic phase that occurs in the weak-disorder, weak-interaction limit.

Introduction In recent years there have been growing interests in the study of localization in interacting many-particle systems with strong disorder [1–3]. In contrast to usual many-body systems that are chaotic and irreversible (i.e. obey thermodynamics description), it is observed that there exist many-body localized (MBL) phases that are non-ergodic and reversible[4]. MBL phases are of interest to the scientific community because of their potential application in manipulating quantum information without dissipation. The problem is difficult theoretically because of its intrinsic nature (strong interaction + disorder), and most of the existing theoretical results are based on numerical studies of one-dimensional (1D) systems.

It is generally accepted that in the ergodic, irreversible phase, the many-body state energy eigenvalues follow the statistics of Random Matrix Theory[5–8] and the energy level spacing $s_n = E_n - E_{n-1}$ obeys Wigner-Dyson law for distribution. On the other hand, s_n follows a Poisson distribution $P(s) = \exp(-s/\lambda)$ in the MBL phase where eigenstates are localized randomly and are uncorrelated, λ is the mean-energy-level spacing which is in general a (smooth) function of E_n . The difference between the two types of distribution can be measured by the ratio of consecutive level spacings $r_n = \frac{\min(s_n; s_{n-1})}{\max(s_n; s_{n-1})}$ introduced by Oganesyan and Huse [9]. Its average value in the ergodic phase (GOE ensemble) is $\langle r \rangle_{GOE} \sim 0.5307$ whereas $\langle r \rangle_{Poisson} = 2\ln 2 - 1 \sim 0.386$ in MBL phase. Thus $\langle r \rangle$ provides a convenient tool that gives an overall estimate of whether the many-body states are localized (MBL) or extended (ergodic). Since then, more sophisticated tools have been developed to study the MBL phase, including energy-resolved $\langle r(E) \rangle$ that computes the average value of r_n over a narrow energy window $E_n \sim E \pm \delta E$ [3], the entanglement entropy [10–15] and non-equilibrium (quench) dynamics [16–19], etc. A Fermi-liquid type phenomenology has also been developed that provides a physical picture of the eigenstates in the MBL phase. In this description, the many-body states can be thought

of as adiabatically connected to a set of localized single-particle orbital [20, 21] or local integrals of motion (*liom*) [22–24]. The main differences between MBL and Fermi liquid states are that (i) the one-to-one correspondence between *bare*- and *quasi*-particles in Fermi liquids are, strictly speaking, restricted only to ground and very low-energy states but there seems to be no such restriction in the MBL states. However (ii), whereas the correspondence between bare- and quasi- particle states are not affected by the presence of other quasi-particles in Fermi liquid theory, the *liom* states may depend strongly on the occupations of other *liom* states when the interaction between particles is strong.

In this paper, we shall study the 1D spin-1/2 XXZ model with random longitudinal on-site magnetic fields B_i . The Hamiltonian is

$$H_{XXZ} = \sum_{i=1}^N (J_\perp (S_i^x S_{i+1}^x + S_i^y S_{i+1}^y) + J_z S_i^z S_{i+1}^z + B_i S_i^z), \quad (1)$$

where S_i^α is the spin(-1/2) operator at direction $\alpha = \hat{x}, \hat{y}, \hat{z}$ at site i and B_i is a random magnetic field at z -direction with magnitude $|B_i| < h$. We note that the model can be mapped onto an interacting spinless fermion model in a random potential *via* a Jordan-Wigner transformation. The Hamiltonian has been studied extensively in the weak/intermediate disorder regime to illustrate the transition between the ergodic and MBL phases[3, 9, 16, 25, 26]. We shall study the strongly disordered regime $h \gg J_\perp$ in this paper.

We note that the total magnetization in z -direction, $S_{tot}^z = \sum_i S_i^z$ is a conserved quantity in the above Hamiltonian and the eigenstates of the system can be classified into sectors with different values of $M = \sum_i (s_i^z + \frac{1}{2})$ which measures the total number of spin- \uparrow particles. The system has also a spin-inversion symmetry which maps the system with M spin- \uparrow particles to the system with $N - M$ spin- \uparrow particles.

To understand the properties of the model in the strong disorder limit we start with considering the limit $J_\perp = 0$.

In this case, the system becomes classical and the eigenstates of the system are all localized. The system has two MBL phases: (1) the paramagnetic phase which occurs in the limit $h \gg J_z$. In this case, the spin S_i^z 's take random values $S_i^z = \pm \frac{1}{2}$ and there is no correlation between spins on different sites. (2) In the opposite limit $h \ll J_z$ the system resides in the spin-glass phase characterized by a spin-glass order parameter defined for any eigenstate $|n\rangle$ of the system,

$$SG(E_n) = \lim_{|i-j| \rightarrow \infty} \langle n | S_i S_j | n \rangle \neq 0. \quad (2)$$

For a finite system with open-boundary condition, the spin-glass order parameter [27] can be measured with i, j being the two endpoints of the spin chain.

To understand the spin-glass order we first consider the limit $h = 0$. In this case, the ground state of the system is anti-ferromagnetically ordered and $SG(E_0) = -1(1) \times 0.25$ for a spin chain with even (odd) number of sites. The first excited states of the system have energy $E_0 + J_z$, corresponding to exciting one domain wall in the system and $SG(E_1) = 1(-1) \times 0.25$, independent of where the domain wall locates. Generalizing the argument, we find that the n^{th} excited states of the system have n domain walls with energy $E_n \sim nJ_z + E_0$ and $SG(E_n) \sim (-1)^{n+1} [(-1)^n] \times 0.25$ for chains with even (odd) number of sites. The degenerate energy levels E_n split into distributions with width $\sim \sqrt{N}h$ centered around E_n when the random magnetic field $h \neq 0$ is added. $SG(E_n)$ decreases when h increases and goes to zero when $h \gg J_z$ where the spin configuration becomes completely randomized. Upon ensemble averaging the two MBL phases are separated by a phase transition that occurs at some critical values $h = h_c$.

We shall study numerically in this paper what happens when a small $J_\perp \ll h$ is added to the system by studying the energy level spacing statistics. Before presenting our results we provide some details of our numerical analysis here. We consider spin-1/2 XXZ spin chains with length $N \leq 16$ and Exact Diagonalization (ED) is used to obtain all eigenstates of our models. We employ open boundary condition in our study. We do not consider $N > 16$ systems in our study because of the limitation of computer power. For each set of parameters characterizing the system, we generate 100 random magnetic field samples to perform disorder averaging except in the $J_\perp = 0$ limit where the system becomes classical and a much larger sampling size can be employed (see below). We shall be interested in energy resolved properties of the system in this paper, and for a given energy E , we compute the expectation value of a variable $\langle \hat{O}(E) \rangle$ by averaging over N_M eigen-states with energies closest to E . The disorder averaging is performed afterward, i.e.

$$\langle \hat{O}(E) \rangle = \left\langle \left(\frac{1}{N_M} \sum_{n; E_n \sim E} \langle n | \hat{O} | n \rangle \right) \right\rangle_{\text{disorder}}.$$

where we took $N_{M=4} = 10, N_{M=6,8} = 100$. When comparing between the model with different sets of parameters, it is convenient to introduce the renormalized energy $\epsilon = (E - E_{\min}) / (E_{\max} - E_{\min})$, where E_{\max} and E_{\min} are the highest and lowest eigen-energy of the system, respectively. We note that the total number of states in a system with M spin- \uparrow particles in N lattice sites is C_M^N and changes rapidly with M . In particular, C_M^N is small for $M \sim 1$ and increases rapidly with M until $M = N/2$. For this reason, we shall restrict our calculations to $3 \leq M \leq 8$ (for size $N = 16$) to ensure better statistics.

The $J_\perp = 0$ limit

We consider first the $J_\perp = 0$ limit where we study numerically the order parameter $\langle SG(\epsilon) \rangle$ to confirm the existence and transition between the paramagnetic and spin-glass phases. In this limit the XXZ model becomes the classical Ising model with random magnetic field on z -direction where a much larger number of random field configurations can be studied. We fix $h = 1$ and consider different values of J_z and $M = 8, 6, 4$ and compute $\langle SG(\epsilon) \rangle$ by averaging over $\sim 10^5$ disorder samples in our study.

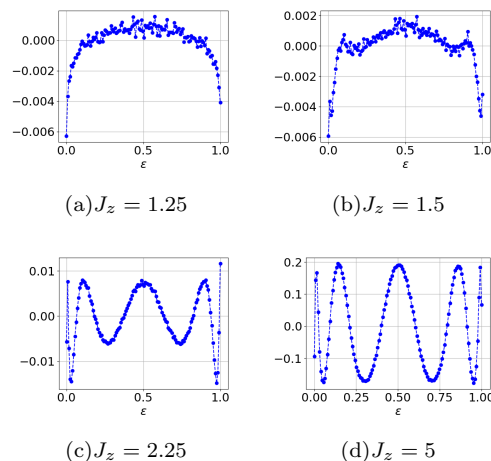


FIG. 1. $\langle SG(\epsilon) \rangle$ for the random field Ising model with system size $N = 16, M = 8$ and $h = 1$. The increase in magnitude of oscillations for increasing $J_z = 1.25, 1.5, 2.25, 5$ are clear.

Our results for $M = 8, J_z = 1.25, 1.5, 2.25, 5$ are shown at Fig.(1). We note that the magnitude of $\langle SG(\epsilon) \rangle$ depends on the density of states at energy ϵ . In the large J_z limit, the oscillation in $\langle SG(\epsilon) \rangle$ with changing energy ϵ is clear. The oscillation vanishes for small J_z .

The magnitude of oscillation $M_{SG} =$ difference between maximum and minimum of $\langle SG(\epsilon) \rangle$ indicates the strength of spin-glass order and is used to estimate the transition point between the paramagnetic and spin-glass phases. We show M_{SG} for different values of M and $J_z \geq 1.5$ (where $\langle SG(\epsilon) \rangle > 0$) in Fig.(2). M_{SG} is fitted

to a function

$$M_{SG} = A(J_z - J_{z,Critical})^\beta \quad (3)$$

to determine the critical point of transition $J_{z,Critical}$. We find $J_{z,Critical} \sim 1.07 \pm 0.05$ for $M = 8$. Similar analysis is also carried out for $M = 4, 6$. The spin-glass order is calculated using $\langle S_1^z S_N^z \rangle - \langle S_1^z \rangle \langle S_N^z \rangle$ as $\langle S_i^z \rangle \neq 0$ in these cases where the system is magnetized. We find $J_{z,Critical} \sim 1.14, 1.33$ for $M = 6, 4$, respectively.

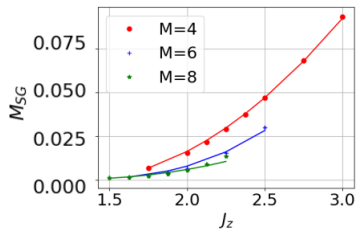


FIG. 2. The magnitude of oscillation $\langle SG(\epsilon) \rangle$ as a function of J_z/h for $M = 8, 6, 4$ (system size $N = 16$). We include only $J_z > 1.5$ datas where $\langle SG(\epsilon) \rangle$ is found to be nonzero.

We note that the critical point $J_{z,critical}$ is increasing when the system moves away from half-filling, indicating that the effect of J_z (or interaction) on spin-glass order is most prominent at $M = 8$ and weakens when the system moves towards smaller value of M . We emphasize once more that the many-body states are localized in both cases, i.e., the paramagnetic and spin-glass phases belong to two different classes of MBL states.

$J_\perp \neq 0$ - existence of an ergodic state between the two MBL phases

We next consider the XXZ model with non-zero J_\perp . We first consider $J_\perp = 0.25$ ($h = 1$) and shall perform our calculations on a system with size $N = 16$ for different values of $M = 3, 4, \dots, 8$ and different values of interaction J_z .

Generally speaking J_\perp drives the system away from localization into ergodic phases. The exchange of spins leads to delocalization (+ creation and destruction) of domain walls leading to the weakening of spin-glass order in the spin-glass phase and to delocalization of spins directly in the paramagnetic phase. Numerically, we confirm that spin-glass order at the strong interaction and strong disorder $J_z, h \gg J_\perp$ limit is much weakened with the introduction of $J_\perp \neq 0$. (see Fig.(3)). However, we have difficulty locating the point of transition between the paramagnetic and spin-glass phases because we cannot arrive at enough numerical accuracy with the small number of disorder samples we considered.

We next examine the energy-level statistics. We first consider weak interaction $J_z = 0.5$. In Fig.(4), we plot $\langle r(\epsilon) \rangle$ for different values of ϵ and M . We note that since both J_\perp and J_z are much smaller than h we expect that the system should remain at the paramag-

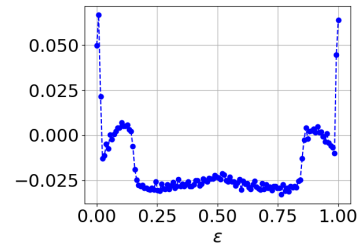


FIG. 3. The oscillation of spin-glass order for a system with $N = 16, M = 8, J_z = 5, J_\perp = 0.25$ and $h = 1$. (150 ensembles)

netic MBL state where all states are uncorrelated (i.e. $\langle r(\epsilon) \rangle \sim 0.38$) through out this region. Instead, we find significant derivation from Poisson statistics behavior in Fig.(4) with $\langle r(\epsilon) \rangle \sim 0.47$ centered around the region $M = 8$ and $\epsilon = 0.5$, indicating that correlations between close-by energy levels is building up around this region.

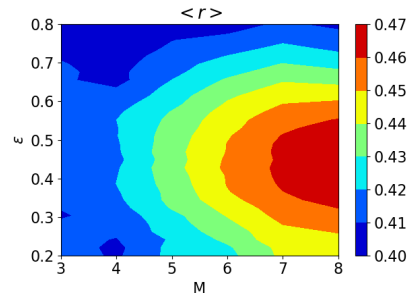


FIG. 4. The ratio of consecutive level spacing $\langle r(\epsilon) \rangle$ for various ϵ and M with $N = 16, J_z = 0.5, J_\perp = 0.25, h = 1$

To understand this behavior better we focus ourselves at $\epsilon = 0.5$ and plot $\langle r(\epsilon) \rangle$ for different values of M and J_z at the fixed energy window $\epsilon = 0.5$ in Fig.(5) with the same parameters $J_\perp = 0.25$ and $h = 1$.

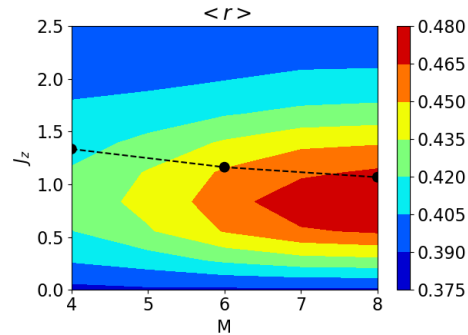


FIG. 5. The ratio of consecutive level spacing $\langle r(\epsilon) \rangle$ with $N = 16, J_\perp = 0.25, h = 1$ and $\epsilon = 0.5$. The black dash line indicates $J_{z,critical}$'s determined in the $J_\perp = 0$ limit.

Interestingly, we find that similar behavior exists, with the derivation of energy levels from uncorrelated (Poisson) behavior strongest at the point $J_z \sim h$, $M = 8$, the energy levels go back to uncorrelated behavior both for stronger and weaker values of interaction J_z and when M deviates from 8. The corresponding value of $\langle r(\epsilon) \rangle$ is around 0.48 at the strongest non-Poisson regime $M = 8, J_z \sim h$. The black dash line indicates $J_{z,critical}$'s determined in the $J_\perp = 0$ limit.

To further understand this behavior we repeat the calculations with different values of $J_\perp = 0.2$ and 0.375 . The results are shown in Fig.(6). We see that the non-Poisson regime expands as J_\perp increases, with $\langle r(\epsilon) \rangle$ moving towards 0.53 at $M = 8, J_z \sim h$ for $J_\perp = 0.375$, suggesting that an ergodic phase emerges around this critical region. The non-Poisson regime shrinks when J_\perp decreases. The critical region is close to the phase transition line separating the paramagnetic and spin-glass MBL phases determined in the $J_\perp = 0$ limit, suggesting that a new ergodic phase is emerging at the critical region between the two different MBL phases when J_\perp becomes nonzero. We shall call it a Many-Body Ergodic phase as it is not analytically connected to the trivial ergodic phase at weak disorder, weak interaction limit (where M is arbitrary and $h \neq J_z$ in general) and appears only at around a region with $J_z \sim h$ and $M \sim N/2$.

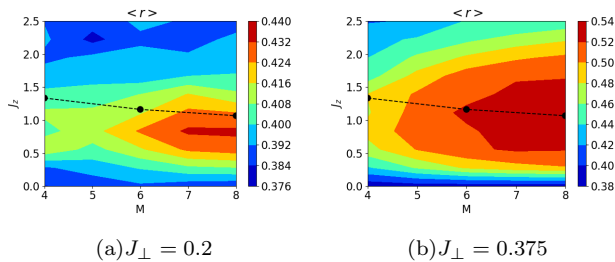


FIG. 6. The ratio of consecutive level spacing $\langle r(\epsilon) \rangle$ with $N = 16, J_\perp = 0.2, 0.375, h = 1$ and $\epsilon = 0.5$. The black dash line indicates $J_{z,critical}$'s determined in the $J_\perp = 0$ limit.

To see whether this critical regime is really approaching an ergodic phase, we also examine the Entanglement Entropy (EE). In the 1D XXZ model we consider here, it is expected that in the limit of large system size N , EE should scale as N in the ergodic phase, and is independent of N in the MBL phase. In Fig.(7), we show the EE for different values of J_z for system size $N = 8, 10, 12, 14, 16$. We fix $M = N/2$ and $h = 1$ in our calculation. For each random field configuration, the EE is computed for P eigenstates with energy closest to the middle of the energy spectrum. The result is then averaged over the P eigenstates and sampled over Q random field configurations. The values of P and Q are determined by the convergence of the calculated value of EE and their values for different system size N are shown in Table.I. We

note from Fig.(7) that the entanglement entropy reaches maximum around $J_z \sim h$ and becomes smaller when J_z moves away from h , consistent with our energy level spacing analysis that an ergodic state is approached when $J_z \sim h$. However, we are not able to obtain the expected scaling behaviours both in the ergodic and MBL phases, suggesting that the sizes of the system we considered are still too small [3].

N	8	10	12	14	16
P	20	50	50	100	500
Q	500	500	500	100	10

TABLE I. The number of states P and random field configurations Q used in calculation of EE for each system size N .

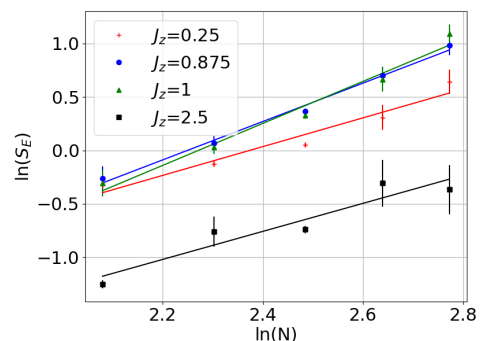


FIG. 7. The log-log plot of the Average Entanglement Entropy of $\epsilon \sim 0.5$ states versus system size N for different values of J_z . We fix $J_\perp = 0.25, h = 1$

Discussion We study in this paper the strongly-disordered regime of the 1D spin-1/2 XXZ chain with random magnetic field along \hat{z} -direction with an aim to investigate the transition between the paramagnetic and spin-class phases. Surprisingly, we find that an ergodic phase emerges at a narrow region between the paramagnetic and spin-glass phases at half-filling ($M = N/2$) in the middle of the energy spectrum ($\epsilon = 0.5$). The ergodic phase emerges around the region with $J_z \sim h$. We call it a Many-Body Ergodic phase as it is not adiabatically connected to the "trivial" ergodic phase in the weak-disorder, weak-interaction limit. This is, to our knowledge, the first time where an emergent ergodic phase between two MBL phases is discovered in exact diagonalization study. It should be emphasized that our finding should be considered as preliminary at this stage. The limitation of our computer power has forced us to work on relatively small size systems ($N \leq 16$) where we were not able to perform a convincing scaling analysis to the $N \rightarrow \infty$ limit. As a result we are not able to conclude with certainty whether the ergodic phase survives in the thermodynamic limit and we are also not able to

pin down precisely whether the ergodic phase is a critical phenomenon that occurs at the boundary between the paramagnetic and spin-glass MBL phases. Large size computer simulations are needed to provide better answers to these questions.

Theoretically, it should be pointed out that renormalization group analysis has suggested that there were no ergodic phase in the critical region between the paramagnetic and spin-glass phases on the disordered 1D transverse-field Ising model [27, 28]. However, the possibility of an emerging ergodic phase between different MBL phases has not been ruled out, in particular when the MBL phases belong to different topological classes [2, 29–31] as in the present case where the *liom* in the paramagnetic phase and spin-glass phase are topologically different (single spins and domain walls, respectively). The prevailing view of a MBL \rightarrow ergodic phase transition is that it is driven by the emergence of resonant clusters. As the strength of randomness is reduced, resonant clusters start to occur more frequently in the system. At the critical disorder strength, a critical cluster grows to encompass the entire system, driving the system into an ergodic phase. Our finding, if correct, suggests a different mechanism of forming ergodic phase when the system is close to the phase boundary between different MBL phases that belong to different topological classes, even in the strong disorder limit. Further theoretical analysis is needed to understand this phenomenon.

acknowledgement

This work is supported by Hong Kong RGC through grant HKUST3/CRF/13G.

-
- [1] R. Nandkishore and D. A. Huse, Annual Review of Condensed Matter Physics **6**, 15 (2015).
- [2] D. A. Abanin, E. Altman, I. Bloch, and M. Serbyn, Rev. Mod. Phys. **91**, 021001 (2019).
- [3] D. J. Luitz, N. Laflorencie, and F. Alet, Phys. Rev. B **91**, 081103 (2015).
- [4] D. A. Huse, R. Nandkishore, and V. Oganesyan, Phys. Rev. B **90**, 174202 (2014).
- [5] Y. Y. Atas, E. Bogomolny, O. Giraud, and G. Roux, Phys. Rev. Lett. **110**, 084101 (2013).
- [6] Y. Avishai, J. Richert, and R. Berkovits, Phys. Rev. B **66**, 052416 (2002).
- [7] K. Kudo and T. Deguchi, Phys. Rev. B **69**, 132404 (2004).
- [8] B. Georgeot and D. L. Shepelyansky, Phys. Rev. Lett. **81**, 5129 (1998).
- [9] V. Oganesyan and D. A. Huse, Phys. Rev. B **75**, 155111 (2007).
- [10] B. Bauer and C. Nayak, Journal of Statistical Mechanics: Theory and Experiment **2013**, P09005 (2013).
- [11] J. A. Kjäll, J. H. Bardarson, and F. Pollmann, Phys. Rev. Lett. **113**, 107204 (2014).
- [12] D. N. Page, Phys. Rev. Lett. **71**, 1291 (1993).
- [13] E. Altman and R. Vosk, Annual Review of Condensed Matter Physics **6**, 383 (2015).
- [14] S. P. Lim and D. N. Sheng, Phys. Rev. B **94**, 045111 (2016).
- [15] V. Khemani, S. P. Lim, D. N. Sheng, and D. A. Huse, Phys. Rev. X **7**, 021013 (2017).
- [16] M. Žnidarič, T. c. v. Prosen, and P. Prelovšek, Phys. Rev. B **77**, 064426 (2008).
- [17] M. Serbyn, Z. Papić, and D. A. Abanin, Phys. Rev. Lett. **110**, 260601 (2013).
- [18] R. Vosk and E. Altman, Phys. Rev. Lett. **110**, 067204 (2013).
- [19] J. H. Bardarson, F. Pollmann, and J. E. Moore, Phys. Rev. Lett. **109**, 017202 (2012).
- [20] T. L. M. Lezama, S. Bera, H. Schomerus, F. Heidrich-Meisner, and J. H. Bardarson, Phys. Rev. B **96**, 060202 (2017).
- [21] S. Bera, T. Martynec, H. Schomerus, F. Heidrich-Meisner, and J. H. Bardarson, Annalen der Physik **529**, 1600356 (2017).
- [22] J. Z. Imbrie, V. Ros, and A. Scardicchio, Annalen der Physik **529**, 1600278 (2017).
- [23] L. Rademaker, M. Ortuo, and A. M. Somoza, Annalen der Physik **529**, 1600322 (2017).
- [24] S. Bera, H. Schomerus, F. Heidrich-Meisner, and J. H. Bardarson, Phys. Rev. Lett. **115**, 046603 (2015).
- [25] A. Pal and D. A. Huse, Phys. Rev. B **82**, 174411 (2010).
- [26] M. Serbyn, Z. Papić, and D. A. Abanin, Phys. Rev. X **5**, 041047 (2015).
- [27] D. A. Huse, R. Nandkishore, V. Oganesyan, A. Pal, and S. L. Sondhi, Phys. Rev. B **88**, 014206 (2013).
- [28] D. Pekker, G. Refael, E. Altman, E. Demler, and V. Oganesyan, Phys. Rev. X **4**, 011052 (2014).
- [29] T. B. Wahl and B. Bri, (2020), arXiv:2001.03167.
- [30] Y. Bahri, R. Vosk, E. Altman, and A. Vishwanath, Nature Communications **6**, 7341 (2015).
- [31] S. A. Parameswaran and R. Vasseur, Reports on Progress in Physics **81**, 082501 (2018).